The Behavior of a Near-Azeotropic Refrigerant Mixture of R-32/R-125 in an Enhanced Tube

K. A. Sweeney and J. C. Chato

ACRC TR-94 April 1996

For additional information:

Air Conditioning and Refrigeration Center
University of Illinois
Mechanical & Industrial Engineering Dept.
1206 West Green Street
Urbana, IL 61801

(217) 333-3115

Prepared as part of ACRC Project 37
Effect of Geometric Variables and R-22 Alternatives on Refrigerant-Side Evaporation and Condensation
J. C. Chato, Principal Investigator

The Air Conditioning and Refrigeration Center was founded in 1988 with a grant from the estate of Richard W. Kritzer, the founder of Peerless of America Inc. A State of Illinois Technology Challenge Grant helped build the laboratory facilities. The ACRC receives continuing support from the Richard W. Kritzer Endowment and the National Science Foundation. The following organizations have also become sponsors of the Center.

Amana Refrigeration, Inc.
Brazeway, Inc.
Carrier Corporation
Caterpillar, Inc.
Dayton Thermal Products
Delphi Harrison Thermal Systems
Eaton Corporation
Electric Power Research Institute
Ford Motor Company
Frigidaire Company
General Electric Company
Lennox International, Inc.
Modine Manufacturing Co.
Peerless of America, Inc.
Redwood Microsystems, Inc.
U. S. Army CERL
U. S. Environmental Protection Agency
Whirlpool Corporation

For additional information:

Air Conditioning & Refrigeration Center
Mechanical & Industrial Engineering Dept.
University of Illinois
1206 West Green Street
Urbana IL 61801

217 333 3115

ABSTRACT

Condensation of a near-azeotropic mixture of 45% R-32 and 55% R-125 has been studied in a microfinned tube. The local behavior of heat transfer coefficient and the pressure drop was found to be a function of both quality and mass flux. The overall enhancement for a microfinned tube was determined to be a result of increased heat transfer combined with an increase in surface area due to the addition of the fins. Another important t result of this study was that the flow regime was found to be an important factor in characterizing the enhancement of the microfinned tube. The effect of the fins on the pressure drop was not readily apparent, but needs further testing in order to be determined.

NOMENCLATURE

Character	Definition
A_s	Surface Area
A_{cs}	Cross-sectional Area
$c_{p,w}$	Specific Heat of the Water
D	Test Section Diameter
$D_{eq,flow}$	Equivalent Flow Diameter
EF	Enhancement Factor
h	Heat Transfer Coefficient
$i_{h,i}$	Enthalpy at heater inlet
i_l	Liquid Enthalpy
i_{lv}	Enthalpy of Vaporization
$i_{ts,i}$	Test Section Inlet Enthalpy
$i_{ts,o}$	Test Section Outlet Enthalpy
k_l	Liquid Conductivity
$\dot{m}_r$	Refrigerant Mass Flow Rate
$\dot{m}_w$	Water Mass Flow Rate
Nu	Nusselt Number
PF	Penalty Factor
$\dot{Q}_h$	Heat Flux in the Heater
$\dot{Q}_{l,h}$	Heat Loss in the Heater
$\dot{Q}_{l,ts}$	Heat Loss in the Test Section
$\dot{Q}_r$	Heat Rejected in the Test Section
$\dot{Q}_w$	Heat Flux in the Water
$\overline{T}_s$	Average Surface Temperature
$\overline{T}_{sat}$	Average Saturation Temperature
$T_{ts,i}$	Temperature at Test Section Inlet
$T_{w,i}$	Temperature at Water Inlet
$x_{ts,i}$	Test Section Inlet Quality
$\left(\frac{\Delta T}{\Delta P}\right)_{sat}$	Change in Temperature with Pressure

INTRODUCTION

In the past few years, the refrigeration industry has gone through significant changes. As the deadline approaches for the complete phase out of chlorinated refrigerants, newer and hopefully better refrigerants are being studied as possible replacements for R-22. One of the possible choices is a mixture of R-32 and R-125. In this report the condensation heat transfer and pressure drop characteristics of a blend of 45% R-32 and 55% R-125 by weight in an internally microfinned tube was studied. By comparing the experimental data to smooth tube correlations, the resulting enhancement due to the use of the microfinned tube was examined.

REFRIGERANT MIXTURES

When two or more refrigerants are combined, the new mixture is significantly different from the pure components. Most refrigerant blends exhibit certain mixture behavior where the temperature changes at a constant pressure as the mixture is condensed or evaporated. This behavior is referred to as a temperature glide, and the refrigerant mixture is referred to as a zeotropic mixture. On the other hand, some mixtures do not exhibit this behavior. They do not have a temperature glide, or the glide is small enough to be ignored. This type of refrigerant is referred to as an azeotropic or near-azeotropic refrigerant. This mixture of R-32/R-125 is one such near-azeotrope, with a temperature glide of approximately 1 °C (1.8 °F)

The properties of azeotropic and near-azeotropic mixtures do not resemble those of the components which make it up. Instead, they are different, and must be determined for each blend. Other researchers have looked at other composition blends of R-32/R-125. Wijaja and Spatz [1995] looked at the behavior of a 50/50% by weight blend. Dobson et al. [1994] looked at both a 60/40% and a 50/50% blend and compared the two. The properties of the 45/55% blend of R-32/125 tested in this study were provided by the manufacturer. From this data, curve fits were created, and were used in the generation of the data. These curve fits are listed in Appendix A.

REFRIGERANT LOOP

The experiments in this study were performed using the apparatus described in detail by Ponchner et al. [1995]. The apparatus consists of a refrigerant loop that includes a water cooled, counterflow condenser test section. The test section is made up of a copper inner tube, surrounded by a plastic annulus, through which the cooling water circulates. Refrigerant is circulated through the refrigerant loop by a gear pump. After the pump, the refrigerant is set to the desired conditions by the use of a series of preheaters. The refrigerant mixture then enters the test section at a known quality and enthalpy. After the refrigerant leaves the test section, it is cooled down to a subcooled liquid by an aftercondenser and a refrigerant to water heat exchanger. It is then recirculated through the pump. Figure 1 shows a diagram of the test apparatus.

The test section in this study is a 9.53 mm (3/8") o.d. tube, containing 60 trapezoidal fins, that are arranged helically inside the tube at an angle of 18°. Figure 2 shows cross sections of this microfinned tube.

Figure 3 shows the details of the test section. At five axial locations, thermocouples measure the exterior wall temperatures. At each axial location, there are four circumferential thermocouple readings, that are averaged to determine a local wall temperature.

This enhanced tube test section has been studied under a variety of conditions and with several pure and mixed refrigerants. Ponchner et al. [1995] looked at the effect of the enhanced tubing on the behavior of pure R-134a. Sweeney et al. [1995] studied the effect that the addition of oil had on the enhanced tube, with R-134a as the refrigerant. In this study, all of the tests were run at a saturation temperature of 35 °C (95 °F). The driving temperature difference between the water and the refrigerant was maintained at 2 °C (3.6 °F). All of the experimental data is listed in Appendix B.

EXPERIMENTAL PROCEDURE

The experimental apparatus mentioned above includes data acquisition software that records several measured values. Measured quantities in the refrigeration loop include temperatures and pressures at both the inlet and outlet of the test section and the preheater. Using these measured values, and curve fits for refrigerant properties, the enthalpy at the inlet of the preheater can be calculated with the following equation.

$$i_{h,i} = i_l(T_{h,i}) \tag{1}$$

Once the heater inlet quality is known, it can be used in conjunction with the measured quantities of heat input, $\dot{Q}_h$, and mass flow rate, $\dot{m}_r$, to determine the test section inlet enthalpy, $i_{ts,i}$.

$$\dot{Q}_h - \dot{Q}_{h,l} = \dot{m}_r(i_{ts,i} - i_{h,i}) \tag{2}$$

Here, the heat loss in the preheater, $\dot{Q}_{h,l}$, is known for each test section, having been determined from single phase testing. During single phase testing, the losses in both the heater and the test section are determined. These losses are functions of the insulation, environment, and the flow conditions. These values are calculated during the single phase tests, and then used during the two-phase calculations.

Now that the test section inlet enthalpy is known, the test section quality can be determined at the inlet, using the definition of quality.

$$x_{ts,i} = \frac{i_{ts,i} - i_l(T_{ts,i})}{i_{lv}(T_{ts,i})} \tag{3}$$

Now all of the necessary information at the test section inlet is known. It is then necessary to look at the entire test section and note that heat transfer is occurring at several locations.. Figure 4 is an illustration of the heat transfer modes that occur in the test section. As one can see in Figure 4, the heat transfer from the refrigerant, $\dot{Q}_r$, can be represented as a combination of the heat across the water section and the heat lost to the environment. Once again, the heat loss in the test section was calculated during single phase testing.

$$\dot{Q}_r = \dot{Q}_w + \dot{Q}_{l,ts} \tag{4}$$

Here, the heat transfer from the refrigerant can be defined in terms of the change in enthalpy across the test section.

$$\dot{Q}_r = \dot{m}_r\left(i_{ts,i} - i_{ts,o}\right) \tag{5}$$

The heat transfer can also be similarly defined as a function of the temperature difference of the water that is flowing across the test section.

$$\dot{Q}_w = \dot{m}_w c_{p,w}(T_{w,o} - T_{w,i}) \tag{6}$$

Using the Equations (4)-(6), the enthalpy at the test section outlet can be determined, given the measured values of water temperatures, and the water flow rate. Then, the test section outlet quality can be determined in a similar way to Equation (3).

In all of the tests conducted in this study, the change in quality across the test section was maintained at below approximately 15%. This was done in order to determine the local behavior of the refrigerant. By averaging the inlet and outlet qualities, the average quality was determined. By maintaining a very small quality difference (less than 15%) across the test section, the researcher was able to accurately determine local behavior. For each test conducted in the present study, the local heat transfer coefficient was found by using the following equation.

$$h = \frac{\dot{Q}_r}{A_s(\overline{T}_{sat} - \overline{T}_s)} \tag{7}$$

In this study, the driving temperature difference used was between the average saturation temperature and the temperature of outer surface of the test section wall, which was approximately the temperature of the inside surface temperature. The average saturation temperature across the test section was calculated as:

$$\overline{T}_{sat} = T_{ts,i} - \left(\frac{dT}{dP}\right)_{sat} \frac{\Delta P}{2} \tag{8}$$

In Equation (8), the relation between the temperature difference and the pressure drop at saturation, $\left(\frac{dT}{dP}\right)_{sat}$, was calculated by using information from the manufacturer.

DIMENSIONLESS PARAMETERS

While the local heat transfer is an important quantity, the data presented here will be in the form of dimensionless parameters. This allows for a more general interpretation of the results. The dimensionless heat transfer used will be the Nusselt number which is defined with the following equation.

$$Nu = \frac{hD}{k_l} \tag{9}$$

For a microfinned tube, the diameter, D, is defined as an equivalent flow diameter. This equivalent flow diameter is defined by the following expression for cross-sectional area.

$$A_{cs} = \frac{\pi}{4}(D_{eq,flow})^2 \tag{10}$$

Because the reason for this study was to find how the microfinned tube enhances the behavior of the refrigerant, it is important to define certain enhancement parameters. In this report, the enhancement factor will be defined as the ratio of the heat transfer of the enhanced tube to the heat transfer of a smooth tube of the outer diameter, operating at the same conditions.

$$EF = \left(\frac{\dot{Q}_{microfin}}{\dot{Q}_{smooth}}\right) \tag{11}$$

This enhancement can be broken down into the actual enhancement due to increased heat transfer, and the enhancement due to the increased area of the microfins. The enhancement factor

can be represented as the heat transfer enhancement multiplied by the area enhancement ratio. For the tube tested here, this area ratio was calculated as 1.62.

$$EF = \left(\frac{h_{microfin}}{h_{smooth}}\right)\left(\frac{A_{microfin}}{A_{smooth}}\right) \tag{12}$$

The heat transfer coefficient for the comparable smooth tube was calculated using the correlation presented by Dobson et al. [1994]. Dobson presented a local heat transfer correlation that was a function of the flow regime.

Along with the heat transfer enhancement of the microfinned tube, there is also a penalty factor, due to the increased pressure drop generated by the fins. Here, the penalty factor is defined as the ratio of the pressure drop found in the microfinned tube to the pressure drop of a smooth tube of the same outside diameter, operating at the same conditions, over the same length.

$$PF = \left(\frac{\Delta P_{microfin}}{\Delta P_{smooth}}\right)_{same\ length} \tag{13}$$

The corresponding pressure drop for the smooth tube was calculated using the correlation proposed by Souza et al. [1995]. This correlation takes into account both frictional and acceleration pressure drops.

HEAT TRANSFER RESULTS

Figure 5 shows the effect of quality on the Nusselt number for all of the mass fluxes tested. This graph illustrates the fact that as quality increases, the heat transfer is increased at each mass flux. Also shown is the effect that as the mass flux increases, the heat transfer is greater at any specific quality.

Now that the behavior of the R-32/R-125 mixture is shown in the microfinned tube, it is important to look next at its behavior in comparison to a smooth tube. Figures 6, 7 and 8 give the enhancement factor, EF, as a function of average quality for low, medium and high mass fluxes respectively.

At a low mass flux of 75 kg-m^2-s (55 klb$_m$/ft^2-hr), the enhancement factor does not vary much with quality. It is also apparent in Figure 6 that the values of the enhancement factor are approximately equal to the area enhancement of 1.62.

But at the medium mass fluxes, as shown in Figure 7, the enhancement factor is a strong function of quality. At the lower qualities, the enhancement factor is relatively high. But as quality

increases, the enhancement factor decreases in value. Then at the higher qualities, the enhancement factor once again increases to a relatively large value. Also apparent in the medium mass flux cases is the fact that as the mass flux increases, the value of the enhancement factor decreases across the entire quality range.

These trends are thought to be due to the flow pattern changes that occur as both the quality and the mass flux increase. The flow patterns discussed here are defined in detail in the report by Dobson et al.[1994]. At low qualities, and at the lower mass fluxes, the predominant flow regime is found to be wavy flow. In this regime, the majority of the liquid is pooled at the bottom of the tube. But there is a thin liquid film that is present around the rest of the tube wall. It is because of this thin film that the fins have a large effectiveness. The result of the high fin effectiveness is the high enhancement factor in this regime.

As quality increases, the flow regime moves from wavy to annular flow. In annular flow, the majority of the liquid is contained in a film around the entire tube wall. At qualities in the range of approximately 0.4 to 0.6, this film is rather thick. The result of having a relatively thick film is a decrease in the enhancement factor in this region of quality. At higher qualities, the film thickness in the annular region decreases and approaches the size of the fins. Because of this, the enhancement factor once again increases to rather high values.

In Figure 8, it is shown that at the high mass fluxes, the enhancement factor curves follow approximately the same trends as in the medium mass flux case. The enhancement factor starts out at a certain value, but then is found to decrease as the quality increases. The difference in the high mass flux cases, is that the enhancement factor does not increase again at high qualities. This can once again be attributed to the flow patterns. At high mass fluxes, and high qualities, the flow is moving into an annular-misty type flow. In this flow pattern, the remaining liquid is found to move in the vapor core. Here, the microfins and the increased area show little effect.

An important detail to note is that the enhancement factors sometimes fall below the area enhancement ratio of 1.62. This fact makes it apparent that at some points, the microfinned tube provides no heat transfer enhancement. In fact, there is actual degradation in the heat transfer, which takes away from the enhancement that the additional surface area provides.

PRESSURE DROP RESULTS

Due to the small pressure drop across the test section, the experimental pressure drop data could only be measured at high mass fluxes. The data points that were taken are presented in Figure 9. It is apparent that the pressure drop is a function of both mass flux and quality. Figure 10 shows the penalty factor as a function of quality for several different mass fluxes. There seems to be only vaguely identifiable trends that can be found, based on this research. Perhaps an important thing to look at in future work is to break down the total pressure drop into the frictional

and acceleration components. This might make trends more obvious, because the enhanced tube should only affect the frictional component of the pressure drop.

CONCLUSIONS

The use of the R-32/R-125 mixture has been studied in an enhanced tube. In this report the heat transfer and pressure drop data of the enhanced tube is compared to a smooth tube with the use of enhancement and penalty factors. The following conclusions can be made as a result of this work:

- The microfinned tube enhances the heat transfer at every point.
- The actual amount of enhancement is a strong function of both quality and mass flux.
- The characterization of the flow regime can be used in combination with the tube geometry to explain the trends in the enhancement factor.
- Part of the enhancement in heat transfer can be attributed to the increase in surface area that is provided by the addition of microfins

Future work in the area of enhanced tubes should take into account the fact that the pressure drop can be broken down into frictional and acceleration components.

REFERENCES

Dobson, M.K., et al., 1994, "Heat Transfer and Flow Regimes During Condensation in Horizontal Tubes", *ACRC Technical Report 57*, University of Illinois at Urbana-Champaign Air Conditioning and Refrigeration Center.

Ponchner, M., et al., 1995, "Condensation of HFC-134a in an 18° Helix Angle Micro-finned Tube," *ACRC Technical Report 75*, University of Illinois at Urbana-Champaign Air Conditioning and Refrigeration Center.

Souza, A.L. and Pimenta, M.M., 1995, "Prediction of Pressure Drop During Horizontal Two-Phase Flow of Pure and Mixed Refrigerants", FED Vol. 210, Cavitation and Multiphase Flow, ASME, 1995, pp. 161-171.

Sweeney, K.A., et al., 1995, "The Effect of Oil on Condensation in a Microfinned Tube", *ACRC Technical Report 87*, University of Illinois at Urbana-Champaign Air Conditioning and Refrigeration Center.

Wijaya, Halim, and Spatz, Mark, 1995, "Two-Phase Flow Heat Transfer and Pressure Drop Characteristics of R-22 and R32/125", *ASHRAE Transactions*, Vol. 101, No. 1, 1995, pp. 1020-1027.

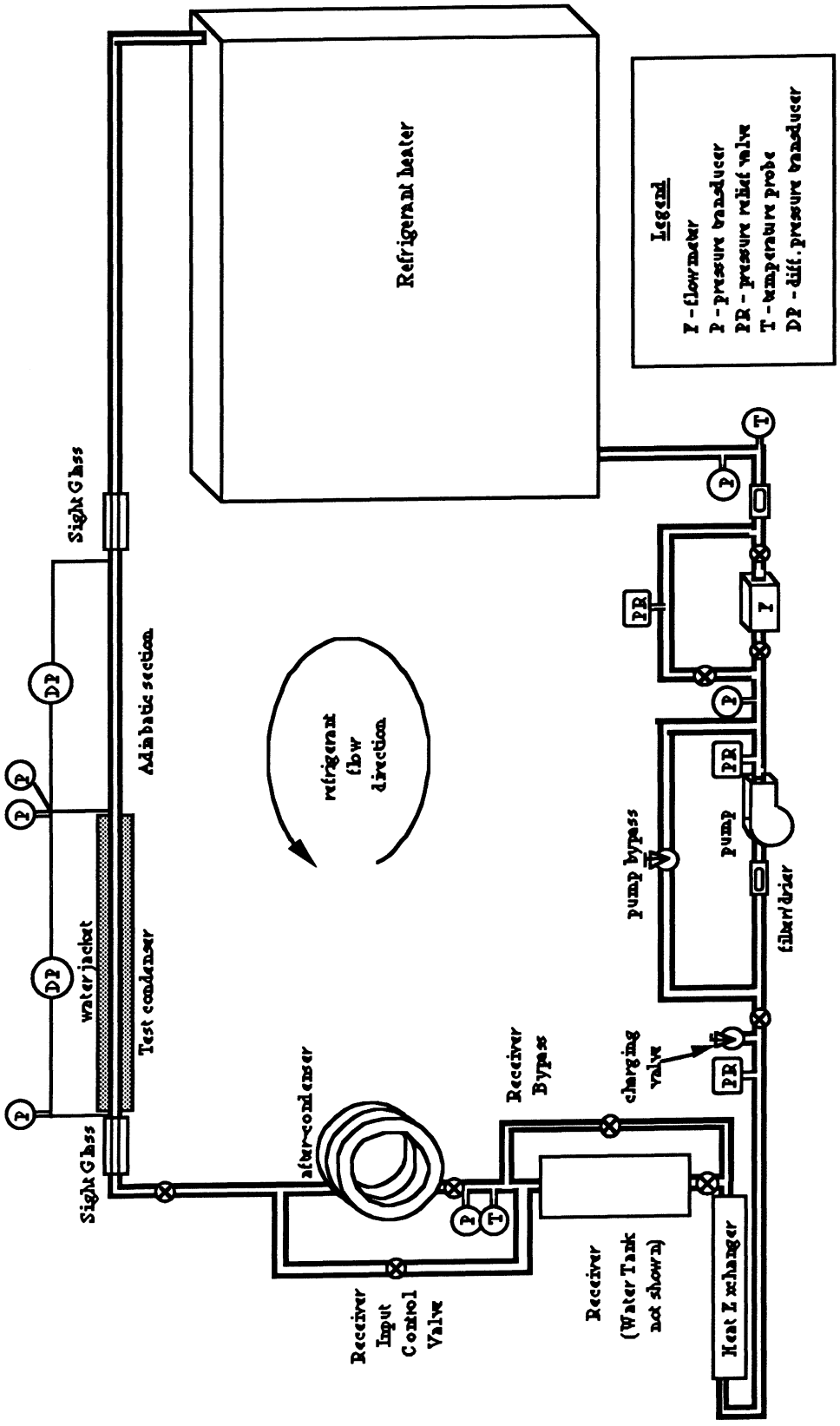

Figure 1: Diagram of the Experimental Apparatus

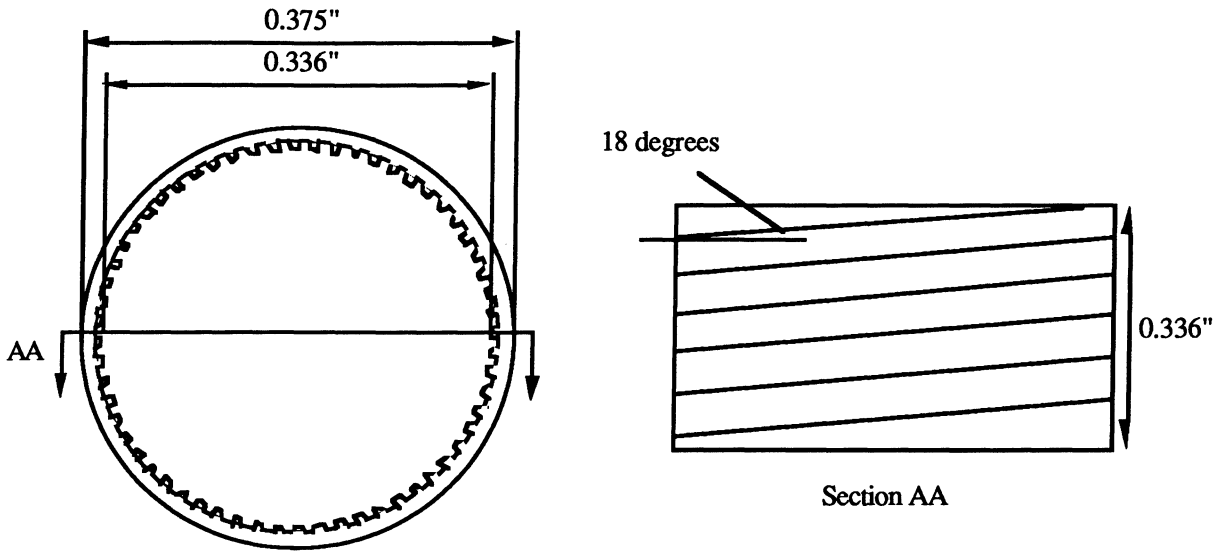

Figure 2: Microfinned Tube Cross Section
Ponchner et al. [1995]

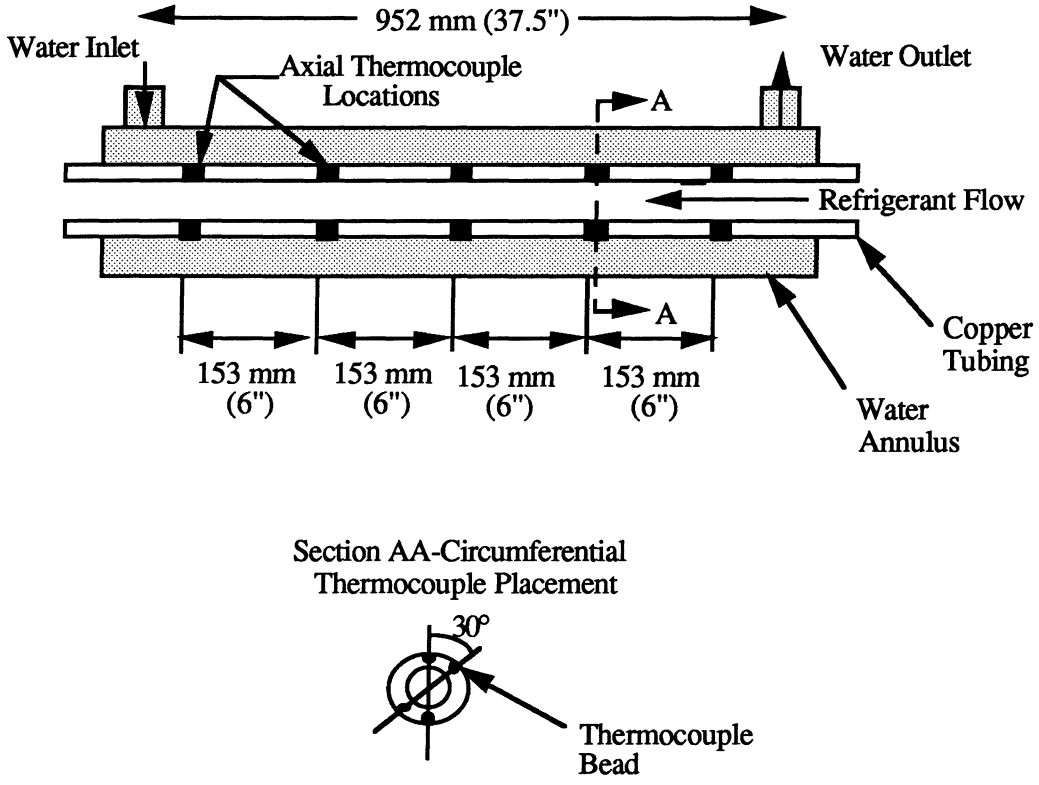

Figure 3: Test Section Schematic

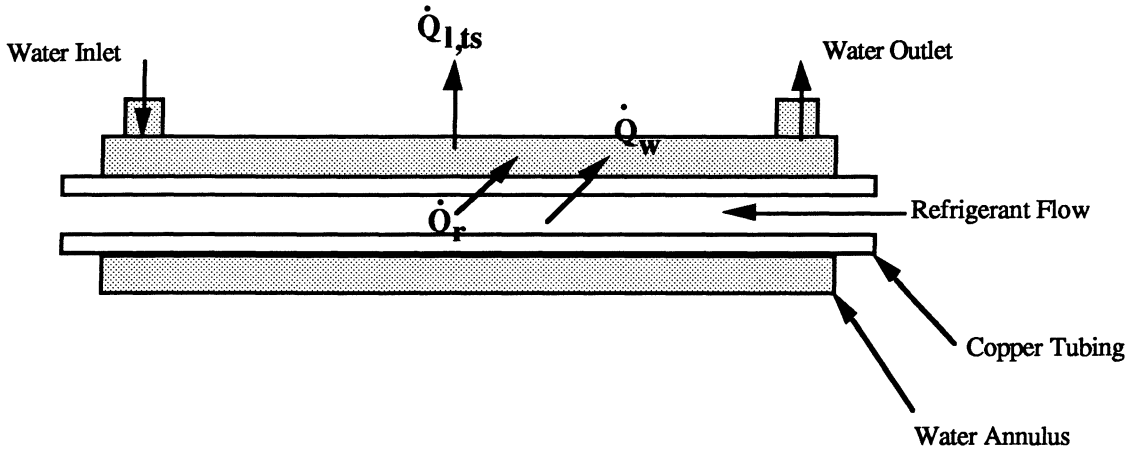

Figure 4: Test Section Heat Transfer Modes

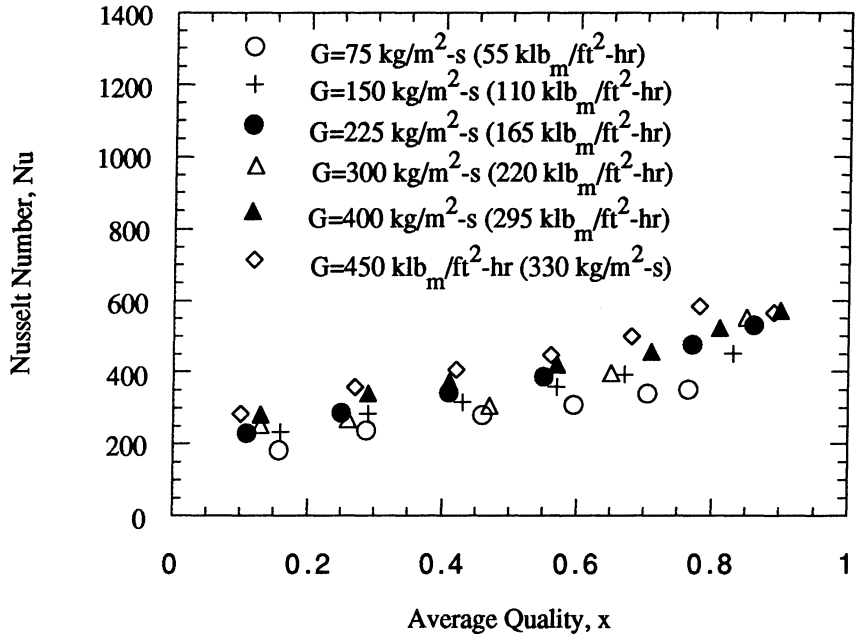

Figure 5: Effect of Quality on Heat Transfer for all Mass Fluxes

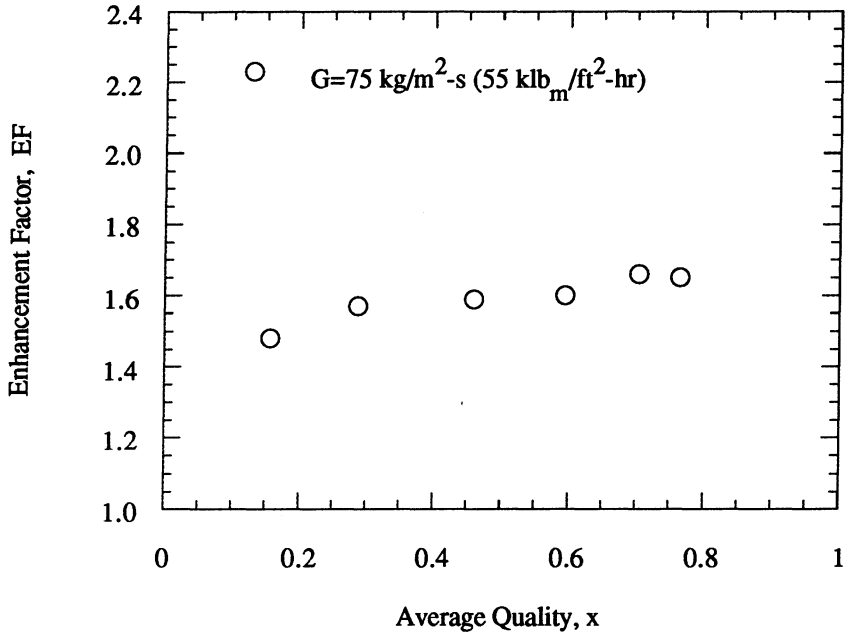

Figure 6: Enhancement Factors for the Low Mass Flux Cases

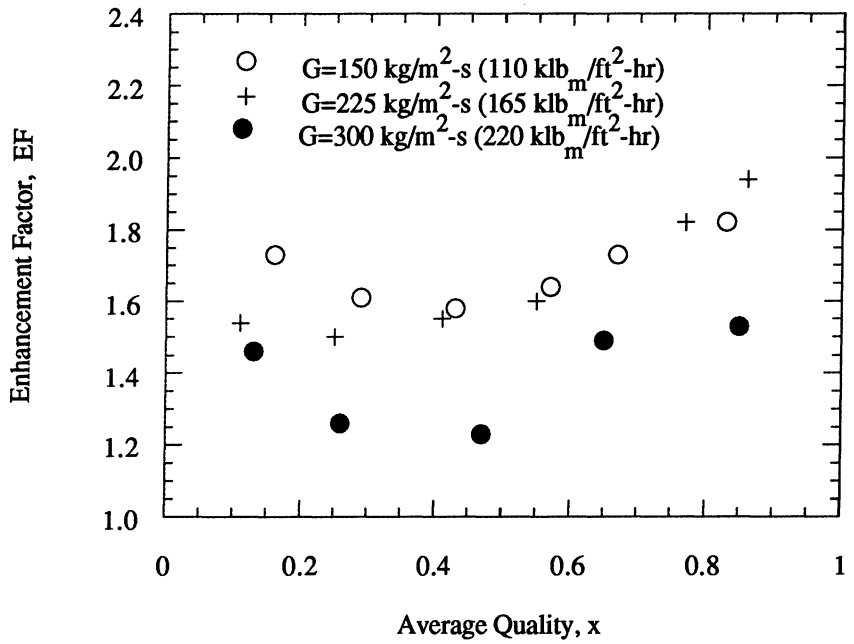

Figure 7: Enhancement Factors for the Medium Mass Flux Cases

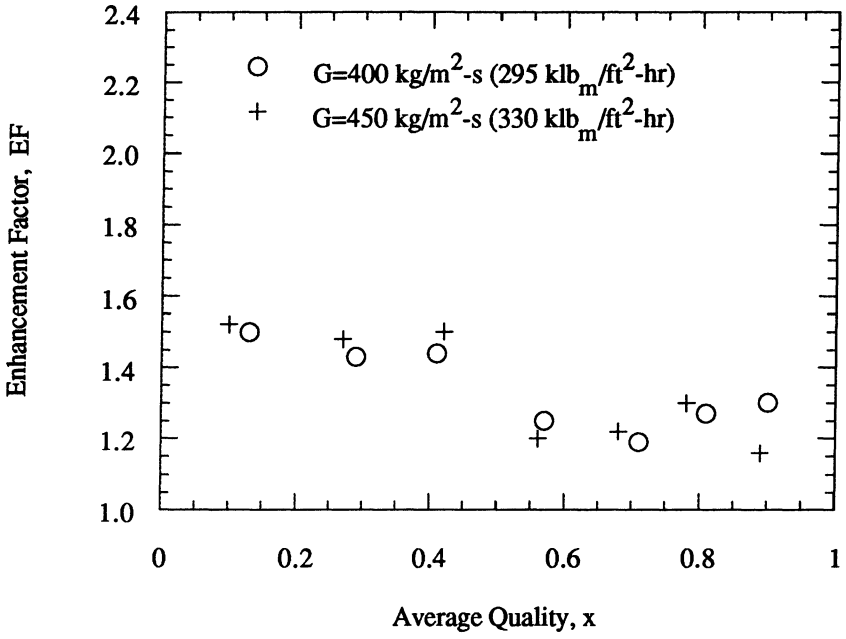

Figure 8: Enhancement Factors for the High Mass Flux Cases

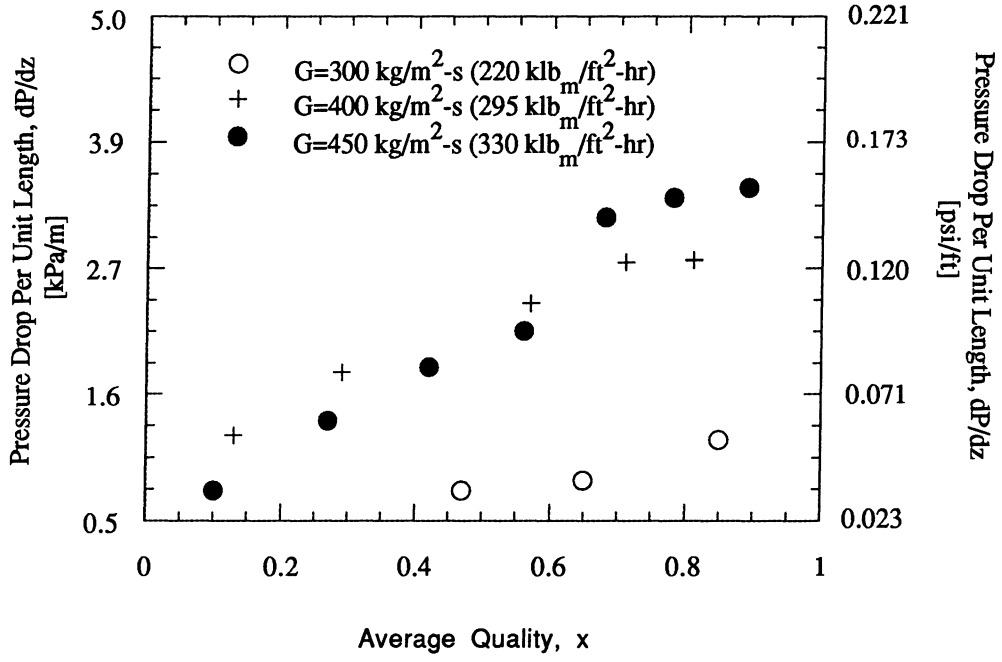

Figure 9: Pressure Drop Per Unit Length

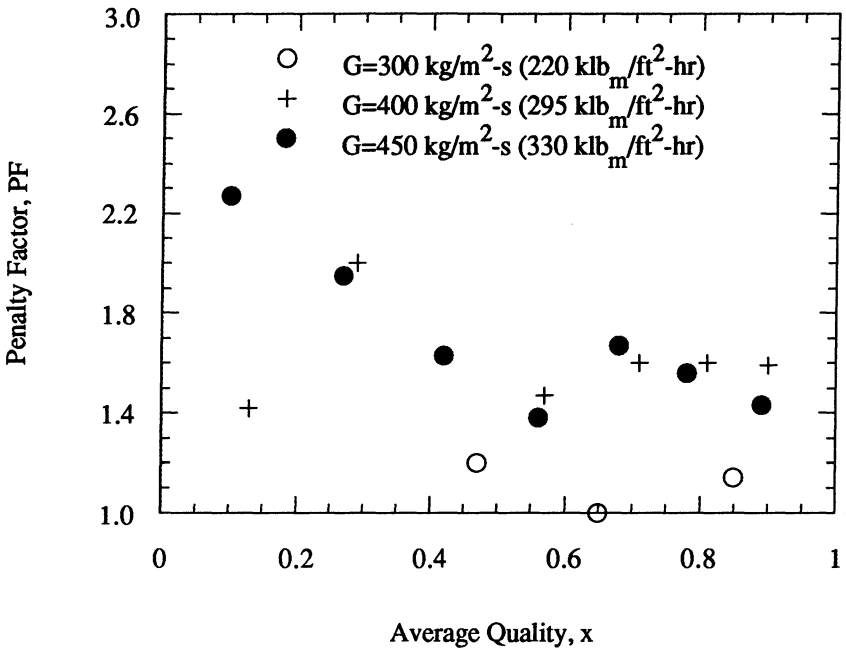

Figure 10: Effect of Quality on Penalty Factor

APPENDIX A

Property Curve Fits for a 45/55 Blend of R-32/R-125

Property	Units	Curve Fit
Saturation Temperature	°C	Tsat=(1/0.026017)*ln(P/843.9)
Liquid Enthalpy	kJ/kg	hf=199.814+1.547*T-0.001343*T^2+7.50311e-5*T^3
Vapor Enthalpy	kJ/kg	hg=415.6589+0.211987*T+0.0023524*T^2-0.000119*T^3
Enthalpy of Vaporization	kJ/kg	hfg=215.84397-1.33502*T-0.003695*T^2-0.000194*T^3
Liquid Viscosity	μPa	μl=(166.0-2.25*T+1.181e-2*T^2-9.20e-5*T^3)/1000000
Vapor Viscosity	μPa	μv=(12.1+8.33e-2*T+1.474e-4*T^2-4.67e-5*T^3+1.08e-6*T^4)/1000000
Liquid Conductivity	W/m°C	kl=(100.1-0.471*T+6.86e-4*T^2-1.29e-5*T^3)/1000
Vapor Conductivity	W/m°C	kv=(12.94+8.885e-2*T-8.14e-4*T^2+5.29e-5*T^3)/1000
Liquid Specific Heat	kJ/kg°C	cpl=1.50625+0.020*T-0.000488*T^2+8.65e-6*T^3
Vapor Specific Heat	kJ/kg°C	cpv=0.77656+0.041617*T-0.001295*T^2+2.0855e-5*T^3
Liquid Density	kg/m^3	rhol=1/(0.0008396+3.997e-6*T-4.6074e-8*T^2+1.33e-9*T^3)
Vapor Density	kg/m^3	rhov=1/(0.03163-0.0009631*T+1.33719e-6*T^2-7.9265e-8*T^3)

These curve fits were generated to best match the data over the range of approximately 0°C (32 °F) to 50 °C (122 °F). The form of the curve fits was chosen to best fit the shape of the data. For the most part, this form was of a third degree polynomial. But, the saturation temperature as a function of pressure was best fit with a logarithmic curve. The curve fits presented here are in SI units, because that is they way that they were received from the refrigerant manufacturer.

APPENDIX B

Experimental Data

Mass Flux [kg/m^2-s]	X	ΔX	Tsat-Twall [C]	h [W/m^2-K]	Nu	DP [kPa]	Flow Regime Inlet	Flow Regime Outlet
79.2	0.16	0.18	1.98	1765	184	0.00	Wavy	Wavy
77.0	0.29	0.22	1.86	2266	237	0.00	Wavy	Wavy
76.1	0.46	0.29	2.01	2673	280	0.00	Annular	Wavy
75.5	0.59	0.31	1.92	2952	309	0.00	Annular	Annular/Wavy
76.1	0.70	0.35	2.00	3256	341	0.00	Annular	Annular
75.6	0.76	0.36	1.97	3357	351	0.00	Annular	Annular
149.0	0.16	0.13	2.18	2228	233	0.00	Wavy	Wavy
150.5	0.29	0.14	1.97	2705	283	0.00	Wavy	Wavy
150.7	0.43	0.16	1.89	3010	315	0.00	Wavy/Annular	Wavy
150.5	0.57	0.17	1.83	3427	358	0.00	Annular	Wavy
150.5	0.67	0.18	1.80	3766	394	0.00	Annular	Annular
150.4	0.83	0.23	1.96	4319	452	0.00	Annular	Annular
230.0	0.11	0.07	1.77	2195	230	0.00	Wavy	Wavy
229.4	0.25	0.10	2.08	2723	285	0.00	Wavy	Wavy
229.4	0.41	0.11	1.86	3288	343	0.00	Annular/Wavy	Wavy/Annular
227.6	0.55	0.12	1.76	3716	388	0.00	Annular	Annular/Wavy
228.1	0.69	0.13	1.83	3907	409	0.00	Annular	Annular
228.6	0.77	0.15	1.79	4548	476	0.00	Annular	Annular
228.8	0.86	0.16	1.81	5068	531	0.00	Annular	Annular
309.5	0.13	0.06	2.03	2404	252	0.00	Annular/Wavy	Wavy
305.7	0.26	0.07	1.96	2555	268	0.00	Annular/Wavy	Wavy
298.8	0.47	0.07	1.76	2920	306	0.93	Annular	Annular/Wavy
292.8	0.65	0.10	1.93	3803	398	1.04	Annular	Annular
299.5	0.85	0.12	1.65	5283	552	1.48	Annular	Annular
403.2	0.13	0.05	1.88	2698	282	0.55	Annular/Wavy	Wavy
404.4	0.29	0.06	1.82	3259	340	1.53	Annular	Annular/Wavy
400.7	0.41	0.07	1.79	3559	373	1.11	Annular	Annular
394.5	0.57	0.07	1.75	4027	421	2.22	Annular	Annular
396.4	0.71	0.08	1.83	4365	457	2.97	Annular	Annular
395.0	0.81	0.10	1.86	4988	523	3.42	Annular	Annular
392.1	0.90	0.10	1.67	5465	572	3.44	Annular	Annular
450.4	0.10	0.05	1.87	2716	284	0.93	Annular/Wavy	Wavy
453.9	0.27	0.06	1.87	3428	358	1.69	Annular	Annular/Wavy
448.8	0.42	0.06	1.76	3893	407	2.27	Annular	Annular
449.6	0.56	0.07	1.87	4288	448	2.67	Annular	Annular
452.2	0.68	0.08	1.92	4771	500	3.91	Annular	Annular
449.9	0.78	0.10	2.01	5582	584	4.12	Annular	Annular
450.1	0.89	0.08	1.73	5427	566	4.23	Annular	Annular